Possible room-temperature signatures of unconventional 4f -electron quantum criticality in YbMn6Ge6–xSnx

Lucas Eichenberger, Arnaud Magnette, Daniel Malterre, Romain Sibille, François Baudelet, Lucie Nataf, Thomas Mazet

Rapid Communications

Possible room-temperature signatures of unconventional 4*f*-electron quantum criticality in $YbMn_6Ge_{6-x}Sn_x$

L. Eichenberger,[1] A. Magnette,[1] D. Malterre,[1] R. Sibille,[2] F. Baudelet,[3] L. Nataf,[3] and T. Mazet[1,*]

[1]*Université de Lorraine, CNRS, IJL, F-54000 Nancy, France*

[2]*Laboratory for Neutron Scattering and Imaging, Paul Scherrer Institut, 5232 Villigen PSI, Switzerland*

[3]*Synchrotron SOLEIL, UR1 CNRS, Saint-Aubin-BP48, 91192 Gif-sur-Yvette, France*

(Received 28 May 2019; revised manuscript received 8 January 2020; published 21 January 2020)

We investigate the Sn composition dependence of the Yb valence and local magnetization in $YbMn_6Ge_{6-x}Sn_x$ ($4.25 \leqslant x \leqslant 5.80$) using x-ray absorption spectroscopy (XANES) and x-ray magnetic circular dichroism at the Yb L_3 edge. In these materials, where Mn is ferromagnetically ordered, we observe a decrease of the Yb valence upon reducing the chemical pressure by Sn doping and a suppression of the Yb magnetic moment for strongly hybridized $4f$ states ($v \sim 2.77$). In the vicinity of the Yb magnetic instability ($x_c \sim 5.23$), a remarkably sharp peak is observed in the composition dependence of the valence and magnetic moment at low temperature, which is reminiscent of enhanced valence and magnetic susceptibilities predicted by recent theories on unconventional quantum criticality. This anomaly is also present in the room-temperature XANES signal, suggesting that rare-earth intermetallics with a magnetized $3d$ sublattice form a distinct group of heavy-fermion metals where the high energy of the exchange interactions can bring quantum criticality up to high temperature.

DOI: 10.1103/PhysRevB.101.020408

Competing interactions can suppress a phase transition to absolute zero temperature, which is commonly known as a quantum phase transition. If the transition is second order, a quantum critical point (QCP) delineates the two ground states. Quantum fluctuations at the QCP induce deep alterations in the finite-temperature properties of the system [1]. In metals, such effects result in strong deviations from the Fermi-liquid behavior or unconventional superconductivity for instance [2,3]. Quantum criticality is being investigated in various materials including high-T_c superconductors, insulating magnets, or heavy-fermion systems [1,4]. The latter are mainly Yb- or Ce-based intermetallics where low-energy scales give access to the QCP using nonthermal control parameters such as chemical doping, pressure, and magnetic field [2,3]. Heavy-fermion quantum criticality is traditionally associated with the rare-earth magnetic instability [2,3], and the ground state results from the competition between Kondo screening and Ruderman-Kittel-Kasuya-Yoshida (RKKY) exchange interactions [5]. In this picture, charge degrees of freedom only play a virtual role since an almost integer valence was thought necessary to stabilize a local moment. As a result, the Kondo temperature T_K of such systems does not exceed ~100 K.

More recently, however, unconventional quantum criticality was observed in several $4f$ materials [2,3]. The most prominent example is β-$YbAlB_4$, where quantum criticality appears completely detached from the Yb magnetic instability [6,7] and occurs for strongly intermediate valent Yb ($v \sim 2.73$ and $T_K \sim 250$ K) [8]. Quantum valence criticality was also found in the related materials α-$YbAl_{1-x}Fe_xB_4$ [9], and has been discussed by various theories including Kondo destruction [10,11] and critical valence fluctuations [12,13].

In $YbMn_6Ge_{6-x}Sn_x$ materials, homogeneous intermediate valent Yb coexists with a magnetized $3d$ sublattice [14–17], while Yb is typically alloyed with nonmagnetic elements in the quantum-critical metals that were mentioned above. The hexagonal $HfFe_6Ge_6$ structure type of the considered materials comprises one site for Mn, one site for Yb, and three sites for the p elements. The Mn sublattice orders magnetically at or above room temperature, and the atomic Mn moment is almost constant throughout the series, close to ~2.2 μ_B [14,16,17]. For $x > 5.23$, Yb is nonmagnetic and the Mn sublattice orders ferromagnetically with the magnetic moments in the basal plane of the hexagonal structure. For $4.25 \leqslant x \leqslant 5.23$, Yb orders and triggers a spin reorientation towards the c axis, resulting in a ferrimagnetic structure. The Sn for Ge substitution, which only occurs at the $2d$ site in the investigated composition range ($4 < x < 6$) [14,17], allows the Yb valence to be changed through negative chemical pressure effects. The (x, T) phase diagram shows that the low-temperature behavior can be described based on a Doniach-like picture [17], but here the Kondo screening competes with, and survives to, the Mn-Yb exchange interaction. In particular, this interaction is much stronger than the usual Yb-Yb RKKY interaction found in Yb-based heavy fermions. This important characteristic results in unprecedented behaviors. Strikingly, the Yb magnetic ordering, which is second order at least for $x \leqslant 5.17$, reaches unusually high temperatures up to $T_{Yb} \sim 125$ K for $x = 4.65$ [17]. Larger Sn contents lead to a decrease of T_{Yb} and the Yb magnetic instability was found to occur near $x_c \sim 5.23$ (Ref. [17]).

In the present work, we investigate the valence and magnetic moment of Yb across the magnetic instability, using,

*Corresponding author. thomas.mazet@univ-lorraine.fr

respectively, x-ray absorption (XANES) and x-ray magnetic circular dichroism (XMCD) at the Yb L_3 edge. Both the Yb valence and XMCD signal decrease upon increasing the Sn content. The XMCD confirms the disappearance of the magnetic ordering of the Yb sublattice for $x > 5.23$, which occurs for strongly intermediate valent Yb ($\nu \sim 2.77$). Our main finding is the observation of a narrow peak close to x_c in the composition dependence of both the Yb valence and the XMCD signal. We suggest these are echoes of quantum criticality of both spin and charge degrees of freedom. This peak persists up to room temperature in the XANES signal, which we attribute to the influence of the magnetized $3d$ sublattice.

Most of the polycrystalline $YbMn_6Ge_{6-x}Sn_x$ samples investigated here ($4.25 \leqslant x \leqslant 5.80$) were used in Ref. [17] where details about their synthesis, crystal, and magnetic properties can be found. The XANES and XMCD spectra at the Yb L_3 edge were recorded using the ODE beamline at the French National Synchrotron Facility (SOLEIL) [18]. The dichroism effect is given by the difference of the x-ray absorption intensities recorded under an applied field of 1.3 T aligned parallel and antiparallel to the beam while keeping constant the beam helicity.

In Figs. 1(a) and 1(b) we show the evolution of the L_3-edge XANES spectrum throughout the investigated composition range at 300 and 5 K, respectively. The main structure at 8.948 keV and the shoulder at 8.941 keV correspond, respectively, to transitions from the initial intermediate valent state to final states of $2p^5 4f^{13}$ (trivalent) and $2p^5 4f^{14}$ (divalent) character, respectively. The intensities of these two structures are thought to be proportional to the weight of the corresponding configurations in the initial state. Details about the fitting procedure can be found in the Supplemental Material [19] together with the whole recorded XANES spectra. As expected from the negative chemical pressure effect associated with the substitution of Sn for Ge, a transfer of spectral weight is observed from the Yb^{3+} component towards the Yb^{2+} component (from $\nu \sim 2.97$ for $x = 4.25$, down to $\nu \sim 2.68$ for $x = 5.80$). However, compositions close to the magnetic instability are characterized by an abnormally high trivalent component at both 5 and 300 K. Notably, measurements on materials with close compositions in the range $5.15 \leqslant x \leqslant 5.20$, that is just below $x_c \sim 5.23$, reveal an intense and narrow peak in the composition dependence of the Yb valence [Fig. 2(a)].

In order to gain information on the local magnetism of Yb, we carried out low-temperature XMCD experiments at the Yb L_3 edge corresponding to the excitation of the $2p_{3/2}$ level. The XMCD signal gives information about the magnetization of the symmetry-allowed final states. Although a quantitative analysis of XMCD spectra using sum rules [20,21] might allow spin and orbital Yb moments to be determined, these sum rules do not apply to $L_{2\text{-}3}$ edges of rare earth so that only qualitative information can be obtained. The $L_{2\text{-}3}$ edges spectra are dominated by dipolar transitions with final states of mainly $5d$ character, but quadrupolar transitions are also possible with smaller probabilities and Yb $4f$ states can be directly probed.

In $3d$-$4f$ intermetallics such as $YbMn_6Ge_{6-x}Sn_x$, the $3d$ Mn-$4f$ Yb indirect exchange interaction is mediated by the

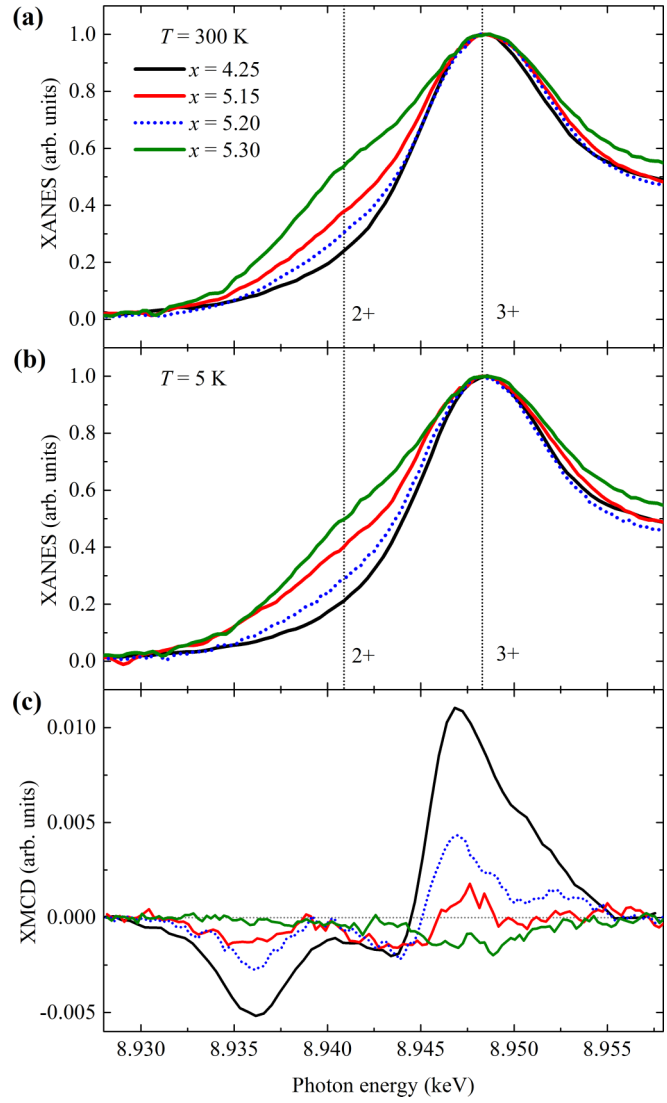

FIG. 1. Yb L_3 XANES spectra for different compositions at 300 K (a) and 5 K (b). The relative intensities of the two structures associated with Yb^{+2} and Yb^{+3} is a direct measure of the Yb valence in the initial state. (c) L_3-edge XMCD spectra at 5 K.

spin-dependent $3d$ Mn-$5d$ Yb hybridization, which yields a negative $5d$ spin magnetic moment (i.e., opposite to the $3d$ Mn moment) at the Yb site. This induced $5d$ moment interacts with the $4f$ spin moment through a local ferromagnetic exchange interaction. In addition, since the spin-orbit constant is positive for a heavy rare earth, the orbital $4f$ moment aligns with the $4f$ spin moment. The net result is an antiferromagnetic coupling between the $3d$ moment of Mn and the $4f$ moment of Yb, as always observed in $3d$-$4f$ intermetallics involving a heavy rare earth [22].

The composition dependence of the low-temperature XMCD spectrum at the L_3 edge is shown in Fig. 1(c). A typical XMCD L_3-edge spectrum of magnetically ordered Yb exhibits three features: one large positive peak at $E \sim 8.948$ keV having a shoulder at $E \sim 8.952$ keV, and two negative ones at $E \sim 8.937$ keV and $E \sim 8.944$ keV. Although the structure at $E \sim 8.944$ keV was sometimes interpreted to result from quadrupolar transitions [23], there

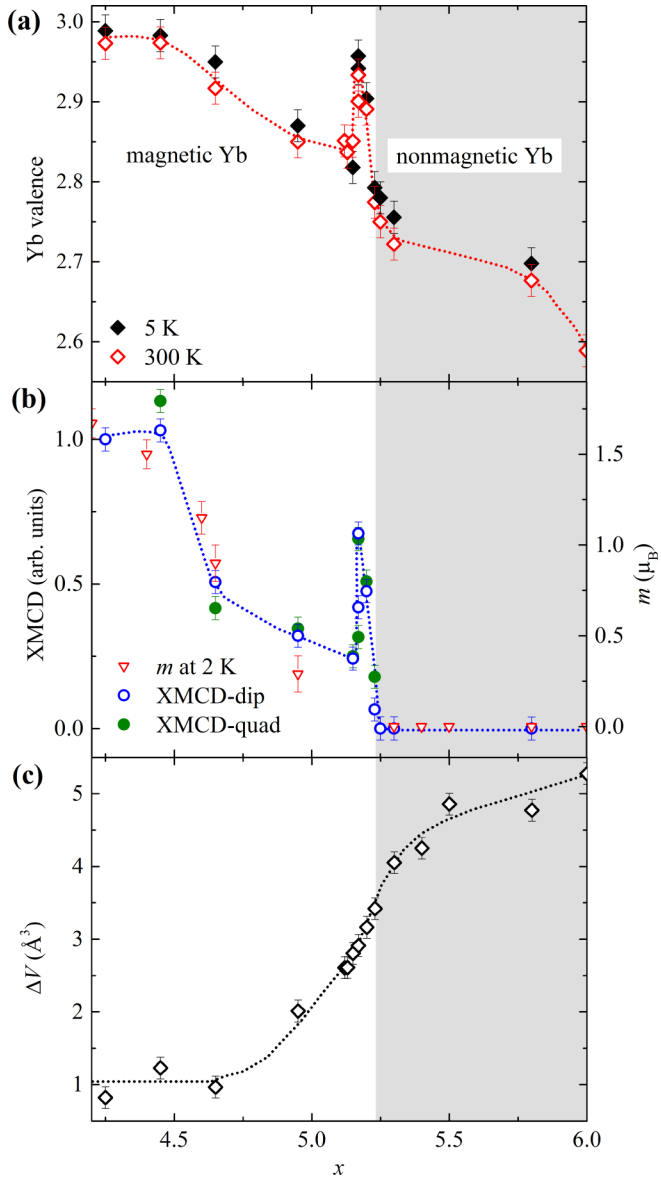

FIG. 2. (a) Composition dependence of the Yb valence at 300 K (red diamonds) and 5 K (black diamonds) extracted from the XANES spectra. The data for $x = 6.0$ come from Ref. [29]. (b) Composition dependence of the dipolar (blue circles) and quadrupolar (green circles) XMCD signals at 5 K (left scale) extracted from the XMCD spectra. In addition, the Yb moment (red triangles) deduced from previous neutron diffraction experiments [17] is reported (right scale). (c) Departure of the room-temperature cell volume from that expected for a fully trivalent Yb (ΔV). The cell volumes were obtained from x-ray diffraction. ΔV was obtained after subtracting a hypothetical trivalent cell volume from the refined cell volumes of $YbMn_6Ge_{6-x}Sn_x$. The hypothetical trivalent volume was obtained by linear interpolation between that of $LuMn_6Ge_2Sn_4$ ($V = 218.49$ Å^3) [28] and that of $LuMn_6Sn_6$ ($V = 235.90$ Å^3) [29].

are now converging evidences that the quadrupolar signal is localized in the pre-edge region [24,25] and thus corresponds to the peak at $E \sim 8.937$ keV.

Besides the quadrupolar contribution, the Yb L_3 XMCD spectra also include two components from dipolar ($5d$) origin [24]. The first one is due to the hybridization with the $3d$ magnetic states of Mn. It is systematically present in the spectra of $YbMn_6Ge_{6-x}Sn_x$ recorded at 5 K because the Mn sublattice creates a nonzero exchange field H_{ex} at the Yb site. This contribution yields the weak negative and broad signal observed for nonmagnetic Yb [$x = 5.30$ in Fig. 1(c)] which persists as the less intense negative peak at $E \sim 8.944$ keV when the other dipolar contribution has grown enough. This second $5d$ contribution is due to the local exchange interaction with the $4f$ spin and yields the large positive structure at high energy. Therefore, the positive dipolar structure and the negative quadrupolar peak are both responsive to the $4f$ moment. The quadrupolar contribution is directly given by peak maximum intensity at $E \sim 8.937$ keV. Because the two dipolar contributions partially overlap, an estimate of the dipolar contribution due to hybridization with the Mn $3d$ states is given by the peak intensity at $E \sim 8.944$ keV, while the dipolar part due to the exchange interaction with the $4f$ states is taken as the positive signal superimposed to that due to hybridization (see [19]).

Figure 2(b) shows the composition dependence of the quadrupolar intensity as well as that of the dipolar contribution due to local exchange with $4f$ states. The XMCD intensity globally decreases with x, and the last trace of $4f$ magnetism is found for $x = 5.23$. Alloys with larger Sn content only present the weak negative dipolar contribution due to the hybridization with the polarized $3d$ states of Mn. These results agree with previous neutron powder diffraction experiments [17] that also located the Yb magnetic instability near $x_c \sim 5.23$, as shown in Fig. 2(b). Our study thus indicates that the Yb valence at the magnetic instability has a strongly mixed character, $v \sim 2.77$, which is similar to that found in α-$YbAl_{1-x}Fe_xB_4$ [9]. Additionally, alloys with x just below x_c present enhanced $4f$ magnetism compared with neighboring compositions, which yields a peak in the composition dependence of the XMCD signal [Fig. 2(b)]. This anomaly occurs for the same compositions as the peak in the composition dependence of the valence, indicating that spin and charge degrees of freedom are intertwined.

The Kondo breakdown and critical valence fluctuation theories both predict enhanced valence susceptibility ($\chi_v = -\frac{\partial v}{\partial \epsilon_f}$) and magnetic susceptibility ($\chi_S = \frac{\partial m}{\partial H}$) in the vicinity of the QCP [12,26,27]. Here, ϵ_f is the energy of the $4f$ level, m is the Yb moment, and, in the present context, H is the exchange field H_{ex} at the Yb site. The latter is assumed to be constant in alloys around $x_c \sim 5.23$. Our data indicate enhanced Yb valence v (at 300 and 5 K) and Yb magnetic moment $m = \chi_S H_{ex}$ (at 5 K), which agrees with these theoretical predictions and strongly suggests the proximity of a QCP. The sharp peak in the composition dependence of the Yb valence is present at room temperature, which indicates that quantum critical effects would manifest themselves at temperatures as high as 300 K. The peak occurs for the same compositions at 5 and 300 K, suggesting that quantum criticality occurs in a narrow range of parameters that does not depend on temperature. In Fe-doped α-$YbAlB_4$, the composition at which the Yb valence crossover occurs was also found insensitive to temperature [9]. We further note that, although the valence v is enhanced near the critical composition, no anomaly is found in the corresponding cell volumes [Fig. 2(c)]. This is consistent with

the nondiverging electronic compressibility $\kappa = -\frac{1}{V}(\frac{\partial V}{\partial P})$ predicted by the critical valence fluctuations theory [27].

We now discuss the possible origin of the quantum criticality in $YbMn_6Ge_{6-x}Sn_x$ materials, in the framework of the Kondo breakdown [10,11] and critical valence fluctuation theories [12,13]. Our results suggest that quantum-critical effects involving both spin and electronic degrees of freedom happen in the immediate vicinity of the Yb magnetic instability, deep inside the mixed-valent regime. In the global phase diagram ensuing from Kondo breakdown physics [11], this behavior can be mapped onto the boundary where Kondo destruction and magnetic transition coincide, that is, between a magnetically ordered state with a small Fermi surface and a paramagnetic state with a large Fermi surface. At the corresponding magnetic QCP, criticality arises from spin fluctuations that are associated with a destruction of the Kondo effect. Alternatively, in the critical valence fluctuation theory, the valence crossover can meet the magnetic transition, in which case the latter becomes first order [13]. It should be noted here, however, that we observe an enhancement of the valence instead of a valence crossover near x_c. In addition, although ferromagnetic (or ferrimagnetic) quantum criticality has already been demonstrated [30] and may be favored by quenched disorder [31], which exists here on the metalloid $2d$ site, it is rare and tends to be avoided. Indeed, the transition often evolves to first order upon approaching zero temperature [31]. Thus, we conclude that, if the critical valence fluctuation theory is considered, the observed phenomena in $YbMn_6Ge_{6-x}Sn_x$ materials would be dominantly driven by valence fluctuations.

A quantum-critical regime can manifest itself up to surprisingly high temperatures related to the energy scales of a given system [32,33]. In Kondo materials with magnetic criticality, T_K is low and the Yb-Yb RKKY exchange interaction is weak. Quantum-critical effects are then limited to the lowest temperature. In mixed-valent materials such as β-$YbAlB_4$ or Fe-doped α-$YbAlB_4$, with $T_K \sim 250$ K [6–9], quantum criticality is perceived up to much higher temperature. In β-$YbAlB_4$ for instance, the resistivity evolves linearly up to temperatures exceeding 40 K [8,9]. In $YbMn_6Ge_{6-x}Sn_x$ materials, the Mn sublattice orders magnetically near 300 K, and the strong Mn-Yb interaction shifts the Yb magnetic instability deep inside the mixed-valent regime. At $x_c \sim 5.23$, ν is measured to be 2.77, which yields T_K of at least ~250 K based on the almost linear scaling between these two quantities [34]. Such Kondo temperature is considerably higher than that of most of the $4f$ quantum-critical materials presently known. At the magnetic instability, the characteristic exchange temperature T_{ex} is of the order of T_K, which corresponds to an exchange field $H_{ex} \sim (k_B T_{ex})/\mu_B$ of several hundreds of Tesla, in agreement with that calculated for similar $3d$-$4f$ intermetallics involving large $4f$ shells [35,36]. This exchange field is one order of magnitude larger than that typically associated with $4f$-$4f$ RKKY interactions, which results in a shift of the Yb magnetic instability towards strongly mixed-valent states. In this regime, charge fluctuations become relevant. In particular, they have a higher energy scale than spin fluctuations. We propose that these considerations explain the persistence of quantum-critical effects at room temperature. An additional effect may come from the disorder (at the metalloid $2d$ site partially occupied by Ge and Sn), which is expected to favor high-temperature quantum criticality [33].

To summarize, in $YbMn_6Ge_{6-x}Sn_x$ the strong exchange field generated by the magnetically ordered Mn sublattice brings the Yb magnetic instability to a strongly mixed valence regime where charge degrees of freedom play a role. Enhancement of both the Yb valence and magnetic moment near x_c very likely result from unconventional quantum critical effects. We anticipate that this system is likely not unique, and we propose that Yb- or Ce-based intermetallics with a magnetized $3d$ sublattice form a distinct group of heavy-fermion metals where the high energy of the Kondo and $3d$-$4f$ exchange interactions renders room-temperature $4f$ quantum criticality a nonexceptional event. A parallel can be drawn with permanent magnets where the interaction with the $3d$ sublattice makes the anisotropy of the $4f$ element relevant at high temperature [37]. The $YbMn_6Ge_{6-x}Sn_x$ series deserves further theoretical and experimental works to extend the present results. In particular, thermodynamic measurements on single crystals and spectroscopic measurements of the Fermi surface as a function of chemical pressure will be important to better address the fundamental aspects of the quantum criticality in this family. Our results open new perspectives in the field of $4f$ strongly correlated metals and more particularly on quantum criticality.

We acknowledge the French Synchrotron facility SOLEIL (Saint-Aubin, France) for the allocated beamtime (Experiments No. 20130845, No. 20140775, and No. 20170707). We acknowledge the financial support of Campus France and the Schweizerische Akademie der Technischen Wissenschaften SATW through the Germaine de Staël funding program. We thank Michel Kenzelmann, Markus Müller, and Ashish Chainani for fruitful discussions.

[1] S. Sachdev, Nat. Phys. **4**, 173 (2008).
[2] H. v. Löhneysen, A. Rosch, M. Vojta, and P. Wölfle, Rev. Mod. Phys. **79**, 1015 (2007).
[3] P. Coleman, *Heavy Fermions: Electrons at the Edge of Magnetism* in Handbook of Magnetism and Advanced Magnetic Materials, edited by H. Kronmüller and S. Parkin (Wiley, New York, 2007), and references therein.
[4] N. E. Hussey, J. Buhot, and S. Licciardello, Rep. Prog. Phys. **81**, 052501 (2018).
[5] S. Doniach, Physica B **91**, 231 (1977).
[6] S. Nakatsuji, K. Kuga, Y. Machida, T. Tayama, T. Sakakibara, Y. Karaki, H. Ishimoto, S. Yonezawa, Y. Maeno, E. Pearson, G. G. Lonzarich, L. Balicas, H. Lee, and Z. Fisk, Nat. Phys. **4**, 603 (2008).
[7] T. Tomita, K. Kuga, Y. Uwatoko, P. Coleman, and S. Nakatsuji, Science **349**, 506 (2015).
[8] M. Okawa, M. Matsunami, K. Ishizaka, R. Eguchi, M. Taguchi, A. Chainani, Y. Takata, M. Yabashi, K. Tamasaku, Y. Nishino,

T. Ishikawa, K. Kuga, N. Horie, S. Nakatsuji, and S. Shin, Phys. Rev. Lett. **104**, 247201 (2010).

[9] K. Kuga, Y. Matsumoto, M. Okawa, S. Suzuki, T. Tomita, K. Sone, Y. Shimura, T. Sakakibara, D. Nishio-Hamane, Y. Karaki, Y. Takata, M. Matsunami, R. Eguchi, M. Taguchi, A. Chainani, S. Shin, K. Tamasaku, Y. Nishino, M. Yabashi, T. Ishikawa, and S. Nakatsuji, Sci. Adv. **8**, 3547 (2018).

[10] Q. Si, S. Rabello, K. Ingersent, and J. Lleweilun Smith, Nature (London) **413**, 804 (2001).

[11] Q. Si and S. Paschen, Phys. Status Solidi B **250**, 425 (2013).

[12] S. Watanabe and K. Miyake, Phys. Rev. Lett. **105**, 186403 (2010).

[13] S. Watanabe and K. Miyake, J. Phys.: Condens. Matter **23**, 094217 (2011).

[14] T. Mazet, H. Ihou-Mouko, D. H. Ryan, C. J. Voyer, J. M. Cadogan, and B. Malaman, J. Phys.: Condens. Matter **22**, 116005 (2010).

[15] T. Mazet, D. Malterre, M. François, C. Dallera, M. Grioni, and G. Monaco, Phys. Rev. Lett. **111**, 096402 (2013).

[16] T. Mazet, D. Malterre, M. François, L. Eichenberger, M. Grioni, C. Dallera, and G. Monaco, Phys. Rev. B **92**, 075105 (2015).

[17] L. Eichenberger, D. Malterre, B. Malaman, and T. Mazet, Phys. Rev. B **96**, 155129 (2017).

[18] F. Baudelet, L. Nataf, and R. Torchio, High Press. Res. **31**, 136 (2011).

[19] See Supplemental Material at http://link.aps.org/supplemental/10.1103/PhysRevB.101.020408 for technical details about the analysis procedures and to see the whole recorded spectra.

[20] B. T. Thole, P. Carra, F. Sette, and G. van der Laan, Phys. Rev. Lett. **68**, 1943 (1992).

[21] P. Carra, B. T. Thole, M. Altarelli, and X. Wang, Phys. Rev. Lett. **70**, 694 (1993).

[22] M. S. S. Brooks, L. Nordström, and B. Johansson, J. Phys.: Condens. Matter **3**, 2357 (1991).

[23] C. Giorgetti, E. Dartyge, C. Brouder, F. Baudelet, C. Meyer, S. Pizzini, A. Fontaine, and R.-M. Galéra, Phys. Rev. Lett. **75**, 3186 (1995).

[24] K. Fukui, H. Ogasawara, A. Kotani, I. Harada, H. Maruyama, N. Kawamura, K. Kobayashi, J. Chaboy, and A. Marcelli, Phys. Rev. B **64**, 104405 (2001).

[25] S. M. Ramos, E. N. Hering, G. Lapertot, F. Wilhelm, A. Rogalev, F. Baudelet, and D. Braithwaite, J. Phys.: Conf. Ser. **592**, 012015 (2015).

[26] J. H. Pixley, S. Kirchner, K. Ingersent, and Q. Si, Phys. Rev. Lett. **109**, 086403 (2012).

[27] S. Watanabe, A. Tsuruta, K. Miyake, and J. Flouquet, J. Phys. Soc. Jpn. **78**, 104706 (2009).

[28] G. Venturini, J. Alloys Compd. **398**, 42 (2005).

[29] L. Eichenberger, G. Venturini, B. Malaman, L. Nataf, F. Baudelet, and T. Mazet, J. Alloys Compd. **695**, 286 (2017).

[30] A. Steppke, R. Küchler, S. Lausberg, E. Lengyel, L. Steinke, R. Borth, T. Lühnmann, C. Krellner, M. Nicklas, C. Geibel, F. Steglich, and M. Brando, Science **339**, 933 (2013).

[31] M. Brando, D. Belitz, F. M. Grosche, and T. R. Kirkpatrick, Rev. Mod. Phys. **88**, 025006 (2016).

[32] A. Kopp and S. Chakravarty, Nat. Phys. **11**, 53 (2005).

[33] D. C. Freitas, P. Rodière, M. Nunez, G. Garbarino, A. Sulpice, J. Marcus, F. Gay, M. A. Continentino, and M. Nunez-Regueiro, Phys. Rev. B **92**, 205123 (2015).

[34] K. Kummer, C. Geibel, C. Krellner, G. Zwicknagl, C. Laubschat, N. B. Brookes, and D. V. Vyalikh, Nat. Commun. **9**, 2011 (2018).

[35] J. P. Liu, F. R. de Boer, P. F. de Châtel, R. Coehoorn, and K. H. J. Buschow, J. Magn. Magn. Mater. **132**, 159 (1994).

[36] E. Belorizky, J. P. Gavignan, D. Givord, and H. S. Li, Europhys. Lett. **5**, 349 (1988).

[37] R. Skomski and J. M. D. Coey, *Permanent Magnetism* (Taylor & Francis, New York, 1999).